Isı Bilimi ve Tekniği Dergisi, 26, 1, 1-8, 2006
J. of Thermal Science and Technology

ISSN 1300-3615

NUMERICAL ANALYSIS OF LAMINAR AND TURBULENT SWIRL FLOWS

Tülin BALİ
Karadeniz Teknik Üniversitesi Mühendislik Fakültesi Makina Mühendisliği Bölümü
61080 Trabzon, bali@ktu.edu.tr

(Geliş Tarihi: 15. 11. 2005)

Abstract: A computational study is conducted to investigate laminar and turbulent swirl flows. The governing equations are solved using the k-ε model and the finite volume method. SIMPLE and SIMPLEC algorithms are comparatively used for pressure correction. Convective terms are discretized through the hybrid differencing scheme. At first, the computer code developed is checked against two problems of which analytical solutions are known from the existing literature, the solid body rotation and the source/sink flow. Then, turbulent flow in a pipe is analyzed. Finally, decaying turbulent swirl flow inside the pipe is examined in detail. Decaying swirl flow is assumed to be generated by the insertion of propeller type generators. The results obtained for this case have been also compared with those obtained experimentally and a good agreement is observed.
Keywords: Numerical, Finite volume method, SIMPLE and SIMPLEC algorithm, Swirl flow, Laminar, Turbulent.

LAMİNER VE TÜRBÜLANSLI DÖNMELİ AKIŞLARIN SAYISAL ANALİZİ

Özet: Sayısal çalışma laminer ve türbülanslı dönmeli akışların incelenmesi amacıyla yapılmıştır. Akış eşitlikleri sonlu hacim metodu ve k-ε türbülans modeli kullanılarak çözülmüştür. SIMPLE ve SIMPLEC algoritmaları basınç düzeltmeleri için karşılaştırmalı olarak kullanılmıştır. Konvektif terimler HDS yöntemi ile diskritize edilmiştir. Geliştirilen bilgisayar kodu ilk aşamada analitik çözümleri bilinen katı cisim dönmesi ve kaynak kuyu akışı problemleri ile test edilmiştir. Daha sonra türbülanslı boru akışı analiz edilmiştir. Son olarak da boru içinde azalan dönmeli akış ayrıntılı olarak incelenmiştir. Azalan dönmeli akışın pervane tipli dönme üretecinin yerleştirilmesi ile üretildiği farzedilmiştir. Bu durum için elde edilen sayısal sonuçlar deneysel sonuçlarla karşılaştırılmış ve iyi bir uyum gözlenmiştir.
Anahtar Kelimeler: Sayısal, Sonlu hacim metodu, SIMPLE ve SIMPLEC algoritmaları, Dönmeli akış, Laminer, Türbülans.

NOMENCLATURE

C_1, C_2	Constants for k-ε turbulent model
C_μ	Constant for turbulent viscosity
D	Diameter of pipe [m]
E	relaxation factor
I_n	Iteration number
K	Turbulent kinetic energy [m^2/s^2]
L	lenght of pipe [m]
P	pressure [N/m^2]
q	volumetric flow rate per unit length of cylinder [m^2/s]
r	radial coordinate [m]
R	Radius of pipe [m]
Re	Reynolds number [=ρVD/μ]
S	source Reynolds number
S_ϕ	source term
u	axial velocity component [m/s]
v	radial velocity component [m/s]
v_*	friction velocity [m/s]
x	axial coordinate [m]
w	circumferential velocity component [m/s]
y	distance from pipe wall [m]

Greek Symbols

χ	von Karman constant
ε	dissipation rate of k
ϕ	dependent variable
Γ_ϕ	exchance coefficient for ϕ
μ	dynamic viscosity [N/ms^2]
ν	kinematic viscosity [m^2/s]
ρ	density [kg/m^3]
σ	turbulent diffusion coefficient
Ω	angular velocity [1/s]

Subscripts

a	inner cylinder
b	outher cylinder
d	decay
eff	effective
i	inlet
m	mean
max	maximum

INTRODUCTION

Having a broad range of applications including chemical and mechanical mixing and separation devices, chemical reactors, combustion chambers, turbo machinery, rocketry, fusion reactors, pollution control devices, etc., swirl flows are used to enhance convective heat and mass transfer. The presence of swirl introduces some favorable changes to the flow, such as increasing the flow paths (but at the expense of increasing energy dissipated by friction), decreasing the free area and introducing an angular acceleration to the fluid flow. In heat exchangers, a swirl generated by twisted types, propellers, fins and wires for low Reynolds numbers is shown to lead to increased heat transfer rates.

Many scientists have investigated the influence of swirl on fluid flow and heat transfer. Kreith and Sonju (1965) investigated the average decay of a tape-induced fully developed turbulent swirl flow through a pipe. Smithberg and Landis (1964) analytically and experimentally studied velocity distributions, friction losses and heat transfer characteristics for fully developed turbulent flow in tubes with twisted tape swirl generators. Bali (1998) numerically and Bali and Ayhan (1999) experimentally studied the decay of swirl behind of propeller type swirl generator and the effects of decaying turbulent swirl flow on heat transfer and pressure drop. Nikjooy and Mongia (1991) presented a numerical study of a confined strong swirling flow. Computations were performed using a differential second-moment closure. The effect of inlet dissipation rate on calculated mean and turbulence fields was investigated. Sampers et al. (1993) carried out local velocity measurements and a numerical analysis using the k-ε model and the Algebraic Stress Model. Hoekstra et al. (1999) carried out an experimental and numerical study of turbulent swirling flow in gas cyclones. The performances of three turbulence closure models were comparatively evaluated based on the experimental results. Yang (2000) applied large eddy simulation (LES) to study the fully developed turbulent pipe flow, in particular, to examine the effects of swirl driven by the rotating wall of the pipe. Mondal et al. (2004) numerically studied turbulent isothermal (non-reacting) swirl flow in a combustor for varying side wall expansion angle and different types of swirl generators using a finite difference method. The standard k-ε turbulence model with logarithmic wall function was adopted for the closure. Wang et al. (2004) used laser Doppler velocimetry (LDV) measurement and large eddy simulation (LES) to study confined isothermal turbulent swirling flows in a model dump combustor.

The aim of this study is to numerically investigate decaying turbulent swirl flow in a pipe. A computer code was developed using the finite volume method. The code was checked against some problems for which analytical data is available in the open literature. The comparison gave a credit to the validity of the code. For the decaying turbulent swirl flows, computational results were compared with the experimental ones and a good correspondence was observed.

MATHEMATICAL MODEL

The transport equations representing the conservation of mass, momentum, turbulent kinetic energy and its dissipation rate is written in a general, usual form for steady state and axisymmetric cylindrical coordinates:

$$\frac{1}{r}\left[\frac{\partial}{\partial x}(\rho ru\phi)+\frac{\partial}{\partial r}(\rho rv\phi)-\frac{\partial}{\partial x}(r\Gamma_\phi\frac{\partial\phi}{\partial x})-\frac{\partial}{\partial r}(r\Gamma_\phi\frac{\partial\phi}{\partial r})\right]=S_\phi \quad (1)$$

where ϕ is a general dependent variable. The corresponding expressions of Γ_ϕ and S_ϕ are summarized in Table 1.

The finite control volume method is used. SIMPLE and SIMPLEC algorithms are employed to correct pressures in the solution (Patankar, 1980; Doormall and Raithby, 1984). Hybrid differencing scheme is used to discretize convective terms while viscous terms are discretized with the central differencing scheme. Computations are conducted using a steady-state axisymmetric elliptic flow solver incorporated with the k-ε turbulent model (Bali, 1998). The turbulent viscosity is determined as $\mu_t = C_\mu \rho k^2/\varepsilon$ and the following values for the empirical constants seen in the equations of the turbulent energy and its dissipation rate are used (Launder and Spalding, 1974; Rodi, 1975): $C_\mu = 0.09,\ C_1 = 1.44,\ C_2 = 1.92,\ \sigma_k = 1.0,\ \sigma_\varepsilon = 1.3$.

RESULTS AND DISCUSSION

In this study, a computer code is developed to study turbulent decaying swirl flow in a pipe. At first, the code is validated for the following problems: Solid body rotation, source-sink flows and turbulent pipe flow.

Solid Body Rotation: Fluid in a cylinder case, rotating with a fixed Ω angular speed around its own axis, acts as a solid body because of viscous frictions. In this case, fluid swirls on a cycle without changing its shape, and there is no shear stress. The velocity field is $u=0,\ v=0,\ w=\Omega r$, and the pressure field is $p=\rho\Omega^2r^2/2$ (Schlichting, 1979). Figure 1 shows the boundary conditions of the solid body rotation.

The geometry with a $0.1x0.1m^2$ has an angular velocity of $\Omega = 10\pi/3$. The solution domain is discretize by a *20x20* uniform grid. Relaxation factor is set to be $E = 2$. A convergence factor of $5x10^{-6}$ needed 34 iterations to reach to convergent solution.

Table 1. Γ_ϕ and S_ϕ expressions.

Conservation of	ϕ	Γ_ϕ	S_ϕ
Mass	*1*	*0*	*0*
Axial momentum	*U*	μ_{eff}	$-\frac{\partial p}{\partial x}+\frac{1}{r}\frac{\partial}{\partial r}(r\mu_{eff}\frac{\partial v}{\partial x})+\frac{\partial}{\partial x}(\mu_{eff}\frac{\partial u}{\partial x})$
Radial momentum	*V*	μ_{eff}	$-\frac{\partial p}{\partial r}+\frac{1}{r}\frac{\partial}{\partial r}(r\mu_{eff}\frac{\partial v}{\partial r})+\frac{\partial}{\partial x}(\mu_{eff}\frac{\partial u}{\partial r})+\rho\frac{w^2}{r}-\frac{2\mu_{eff}v}{r^2}$
Circumferential momentum	*W*	μ_{eff}	$-\frac{\rho vw}{r}-\frac{1}{r}\frac{\partial}{\partial r}\left(\mu_{eff}w\right)+\frac{\mu_{eff}}{r}\left(\frac{\partial w}{\partial r}-\frac{w}{r}\right)$
Turbulent kinetic energy	*K*	$\frac{\mu_{eff}}{\sigma_k}$	$G_k^*-\rho\varepsilon$
Turbulent dissipation rate	ε	$\frac{\mu_{eff}}{\sigma_\varepsilon}$	$\frac{\varepsilon}{k}(C_1G_k^*-C_2\rho\varepsilon)$
*) $G_k=\mu_{eff}\left\{2\left(\frac{\partial u}{\partial x}\right)^2+2\left(\frac{\partial v}{\partial r}\right)^2+2\left(\frac{v}{r}\right)^2+\left(\frac{\partial w}{\partial r}-\frac{w}{r}\right)^2+\left(\frac{\partial w}{\partial x}\right)^2+\left(\frac{\partial u}{\partial r}+\frac{\partial v}{\partial x}\right)^2\right\}$			

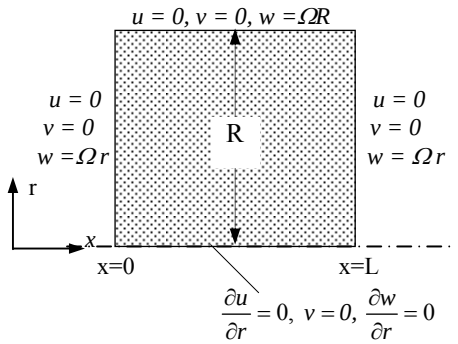

Figure 1. Solid body rotation.

Figure 2 shows circumferential velocity and pressure variations with corresponding analytical solutions. w^* and p^* are non-dimensional circumferential velocity and pressure and they define as $w^*= w/\Omega R$, $p^*= 2p/\rho\Omega^2r^2$. As seen in Figure 2, analytical and numerical solutions are in a good agreement.

Source-Sink Flows : The second test problem is the laminar source-sink flow. The problem geometry consists of two interconnected cylinders rotating with a fixed Ω angular velocity on the same axis. Depending on the flow direction, the inner and outer cylinders are defined as a source or a sink. Neglecting axial variations, analytical solutions were obtained by Hide (1968) for the source-sink flows. The source Reynolds number is given as $S \equiv q/2\pi\nu$, where q is the volumetric flow rate entering from the unit length of the cylinder. Analytical solution, in a stationary cylindrical coordinate system, is given as (Hide,1968):

$$v = q/2\pi r, \quad u = 0,$$

$$w = \frac{\Omega}{\left(R_b^{S+2}-R_a^{S+2}\right)}\left[\frac{R_b^2R_a^2\left(R_b^S-R_a^S\right)}{r}+\left(R_b^2-R_a^2\right)r^{S+1}\right] \quad (2)$$

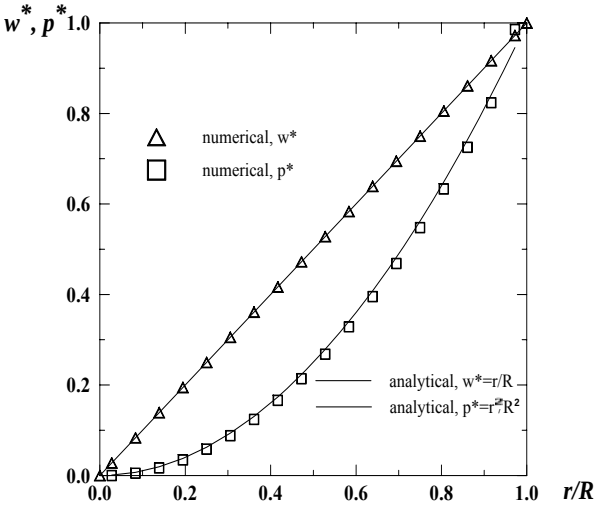

Figure 2. Circumferential velocity and pressure distributions on radial direction ($\Omega=10\pi/3$).

The flow was examined in two different cases with *S=10* and *S = -10*. *S = 10* represents the source-sink flow while *S = -10* represents the sink-source flow. Figure 3 depicts geometry of these flows and relevant boundary conditions.

A 15x20 uniform grid is generated. The following data are used. R_a *= 0.02m,* R_b *= 0.08m* and *L = 0.1m*. Angular velocity is $\Omega = 2\pi$. Relaxation factor is taken to be *2* for *S = 10*, and 5 for *S = -10*. A convergence criterion of $5x10^{-5}$ is used for each equations. For *S = 10*, converged solutions are obtained in 34 iterations, while 74 iterations are needed for *S = -10*. Figure 4 shows the variation of non-dimensional circumferential velocity distribution in the radial direction for *S = 10* and *S = -10*. Non-dimensional circumferential velocity in the rotating coordinate

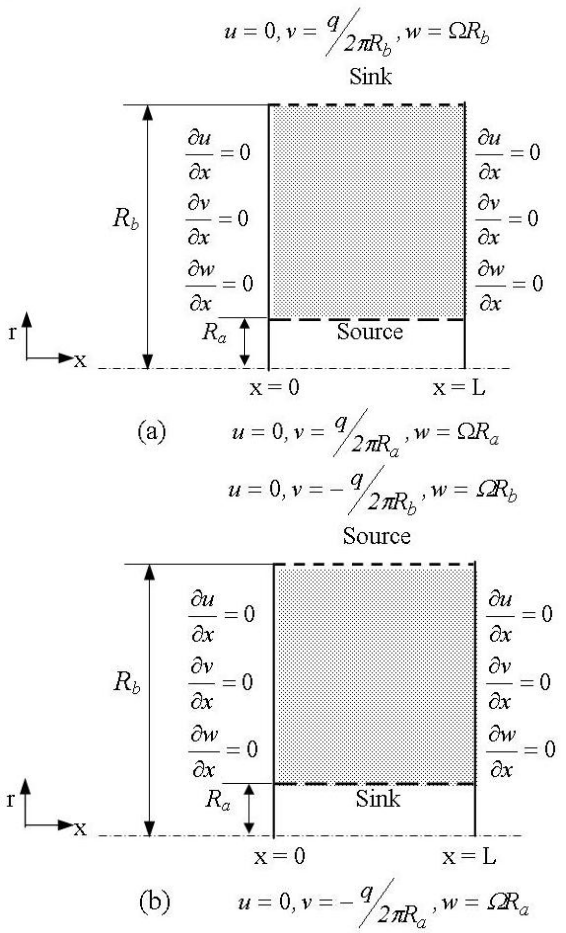

Figure 3. Source-sink flows and boundary conditions (a) *S = 10*; (b) *S = -10.*

system defines as $w^* = (\Omega r - w)/\Omega R_b$. As seen the numerical results are found to be consistent with the analytical results given by Eq. (2). At *S = 10,* circumferential velocity increases from the source and reaches the level in the sink by decreasing in the boundary layer near the sink. In *S = -10,* the maximum circumferential velocity occurs nearly over the sink and reaches the level in the sink by decreasing in the thin boundary layer.

Turbulent Pipe Flow: In this part, the problem of turbulent flow in a pipe is considered. Turbulence is closed with the k-ε model. The fluid enters the pipe with a uniform velocity and flow continues through the pipe. Figure 6 shows the flow geometry and related boundary conditions.The turbulence quantities at the pipe entrance are calculated as follows (Chang et al., 1991):

$$k_i = 0.003u^2, \quad \varepsilon_i = C_\mu k_i^{3/2} / 0.03R \qquad (3)$$

A pipe with a diameter of *0.2m* and a length of *12m* is chosen. A non-uniform grid consisting of 25x15 points in the axial and radial directions, respectively; is used. Here SIMPLEC algorithm, which has been proven to be computationally effective, is preferred. A convergence criterion of 10^{-3} is chosen. The relaxation parameter is chosen to be 9 for all the equations.

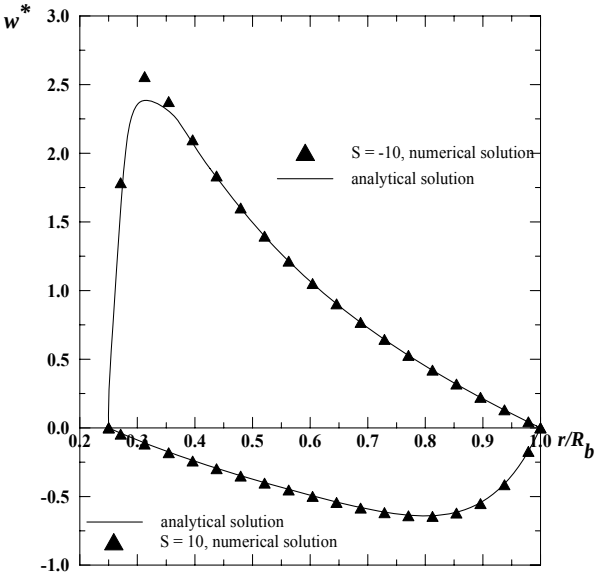

Figure 4. Radial velocity distributions for *S = 10* ve *S = -10.*

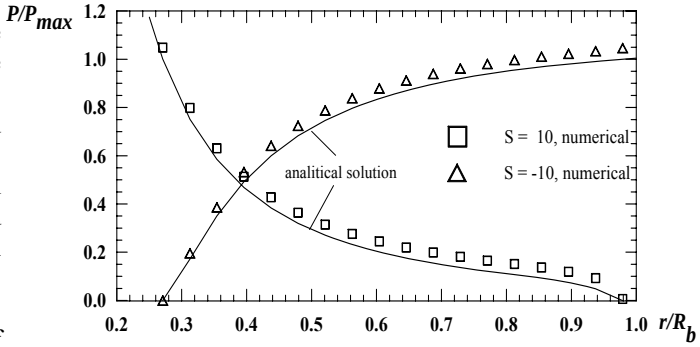

Figure 5. Pressure distributions for source-sink flows.

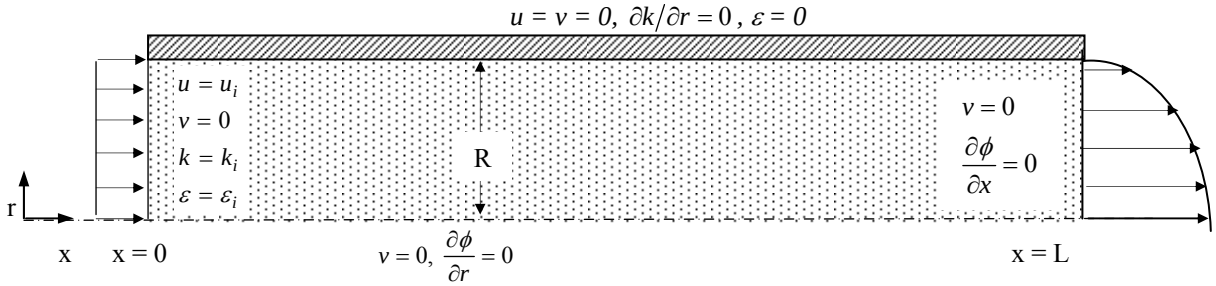

Figure 6. Schematic of turbulent flow in a pipe and boundary conditions.

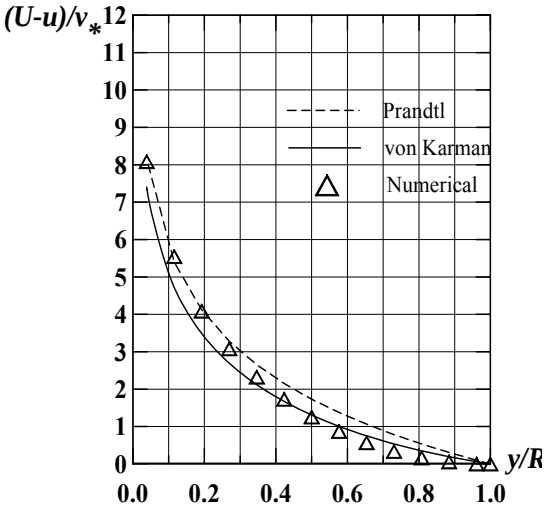

Figure 7. Logarithmic velocity distribution law for smooth pipe.

Figure 7 shows the comparison of the logarithmic wall law, the non-dimensional velocity profiles in laminar sublayer and the turbulent boundary layer. Prandtl and von-Karman universal velocity distribution law expressions are given as follows, respectively (Schlichting, 1979). Symbols *U* and *y* are defined as: $U = max(u),\ y = R\text{-}r$.

$$Prandtl\ :\ U-u = 5.75 v_* \log\frac{R}{y} \tag{4}$$

$$von\text{-}Karman:\ \frac{U-u}{v_*} = -\frac{1}{\chi}\left\{ ln\left[1-\sqrt{1-\frac{y}{R}}\right]+\sqrt{1-\frac{y}{R}}\right\}$$

Figure 8 illustrates optimization of the relaxation factors according to the iteration number needed for converged solutions for the problems considered above.

Decaying Swirl Flow: Swirl decaying through the pipe for twisted turbulators was experimentally examined by Kreith and Sonju (1965). Initial swirl for twisted turbulator is given as:

$$w^*(r,0) = H^{-1}\left\{6.3\left(r/R\right) - 0.013\left[1.1-\left(r/R\right)\right]^{-2.68}\right\} \tag{5}$$

where w^* is non-dimensional circumferential velocity, *H* is the non-dimensional characteristic length of the turbulator and *r/R* is the non-dimensional radial coordinate.

Figure 9a shows the axial velocity profile at the entrance. Eq.(5) defines the circumferential velocity, and the radial velocity is taken as zero at the entrance. Distribution of circumferential the velocity given in Fig. 9b is obtained from the experimental data and the deviations resulting from the secondary flow effects are shown in the graphic. The turbulent kinetic energy and kinetic energy dissipation are determined by Eq.(3). The radial velocity in the pipe axis and exit is taken as zero. The pipe was long enough to provide the derivative boundary condition at the exit. No-slip condition is assumed at the pipe wall. Axial velocity and turbulence-related values near the wall was calculated with the wall functions and the balance equation.

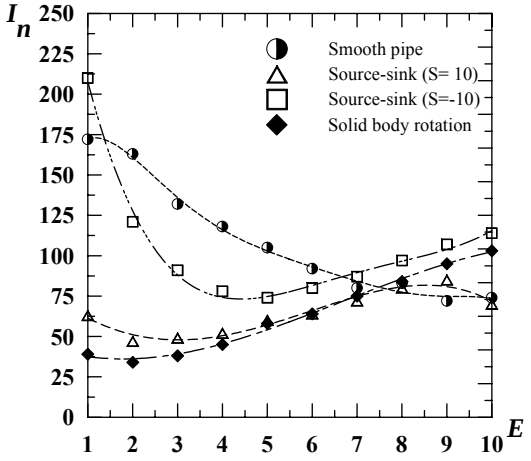

Figure 8. Variation of iteration number with relaxation factor for different flow types considered.

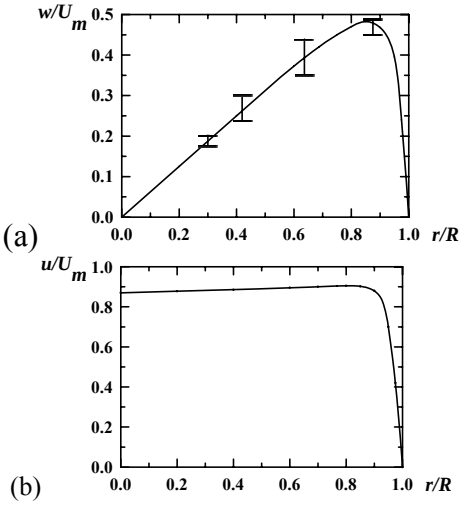

Figure 9. Distributions of initial velocities for *H = 10* [1]; (a) axial, (b) circumferential.

Pipe diameter is *0.0254m* and the pipe length is *120D*. A uniform grid structure with 50x20 points at axial and radial directions is defined which is proven to present grid-independent results. A longer pipe (120D) than that of Kreith and Sonju (1965) (100D) is prescribed in order to define the regarding boundary conditions at the pipe exit more accurately. Relaxation factor is defined as *8.* The convergence criterion is defined as 5.10^{-2} for the turbulent kinetic energy dissipation, ε while it is 10^{-4} for the remaining variables. Figure 10 shows the radial distributions of the circumferential velocity through pipe for Re=48000 and initial swirl number of 0.387. The experimental data of Kreith and Sonju (1965) is included in the figure. As seen, the experimental and numerical results agreed well when the swirl is decayed (i.e. for higher values of x/D) except near the wall, which gives a

credit to the validity of the computer code developed here. Decay of swirl through the pipe was calculated as $W_d = (W_m/W_{in})$ and shown in Fig. 11. Again, the correspondence between the numerical and experimental results (Kreith and Sonju, 1965) are found to be adequate.

Decaying Swirl Flow with Propeller Type Swirl Generator: In this final part of the study, we investigate both experimentally and numerically the effects of swirl flow generated by the propeller type swirl generator on fluid flow. The dimensions of the test section are 54.7mm diameter, 2m length. Air is used as the test fluid. Velocity distributions behind the swirl generator are measured using a hot-wire anemometry (x=0mm, x=120mm, x=620mm and x=1430mm) for the Reynolds numbers of 7491, 13948 and 27036. Measured axial and tangential velocity distributions are taken as the inlet velocity boundary conditions. The inlet values of k and ε were taken from Eq. (6). Since the computational domain is extended to an axial distance of 36.5 diameter of the inner pipe, the outflow boundary conditions are assumed to be fully developed in the calculations and a non-uniform grid with *40x13* points is used. At symmetry axis, for all primitive variables (not v), axial symmetry boundary condition is given as: $\partial\phi / \partial x = 0$; $\partial\phi / \partial r = 0$, $v = 0$. Turbulence kinetic energy and its dissipation are determined at the pipe inlet as (Chang et al., 1991):

$$k_{in} = 0.003u^2 \quad , \varepsilon_{in} = C_\mu \, k_{in}^{1.5} / 0.03R \tag{6}$$

From the engineering interest, it is important to determine the decay rate of the swirl number along the pipe. The local swirl number which is the ratio of tangential to axial momentum flux at a cross section can be defined as (Senoo and Nagata, 1972):

$$m = \int_0^R uwr^2 dr \Big/ \int_0^R u^2 r dr R \tag{7}$$

Numerical results predicted here and the experimental measurements for velocity distributions are shown in Fig. 12. It is shown that the profiles of axial and tangential velocity profiles at various locations for Re = 13948 and initial swirl number of 0.5. Calculations were performed to compare with the experimental results at x=0mm, x=120mm, x=620mm and x=1430mm and a good agreement was found. The flow was initially axisymmetric, but the axisymmetry decayed much more rapidly than the swirl. In each case, after a sufficient distance, the swirl profile was in good agreement with that expected from the axisymmetric computation.

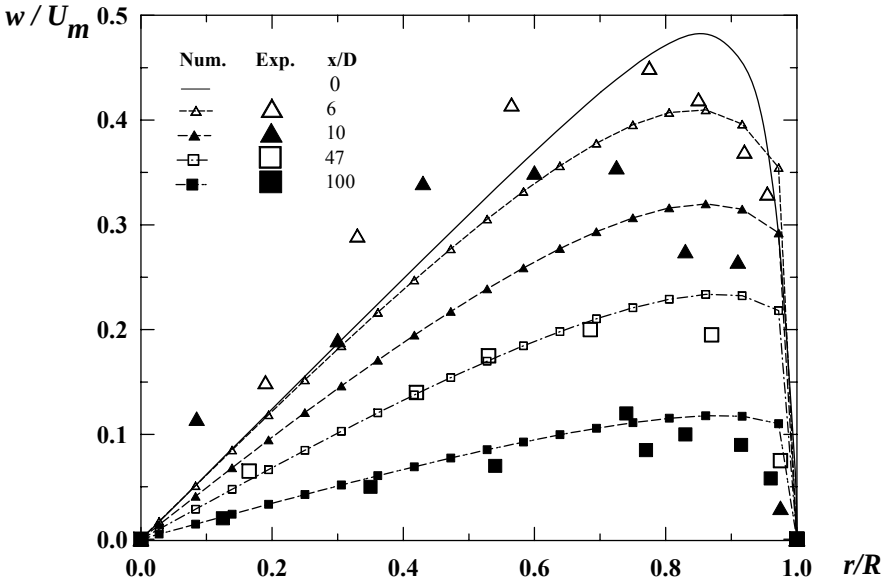

Figure 10. Distributions of circumferential velocity in radial direction through pipe for Re = 48000.

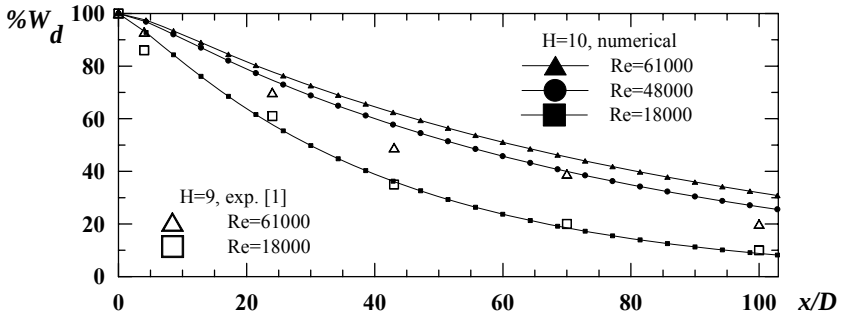

Figure 11. Decay of swirl through the pipe.

Figure 13 shows the variation of the local swirl number with relation to different Reynolds numbers. The data of Kitoh (1991) are also included in Figure 13. In Kitoh's experiments, the swirl was generated by the guide vanes and smaller swirl intensities were studied. The present data as well as Kitoh's data show that the swirl intensity decays approximately exponentially with the axial distance. It was also found that the swirl number increases with the increasing Reynolds number. Since the swirl number decreases along the pipe, the highest decrement of the swirl number occurs at Re=7491.

Finally, it should be noted here that a grid refinement study is carried out for each of the above cases. For each case, the grid size chosen is proven to suggest grid-independent results.

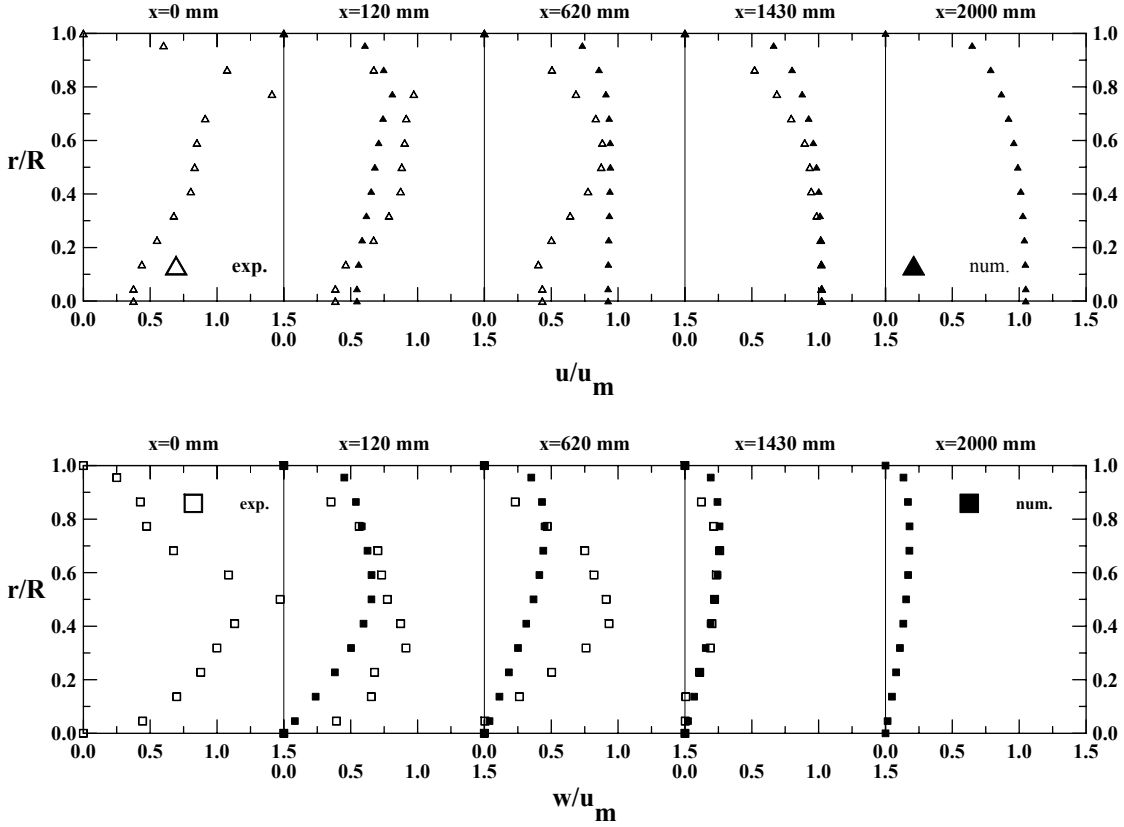

Figure 12. Axial and tangential velocity distributions at the pipe downstream for Re = 13948.

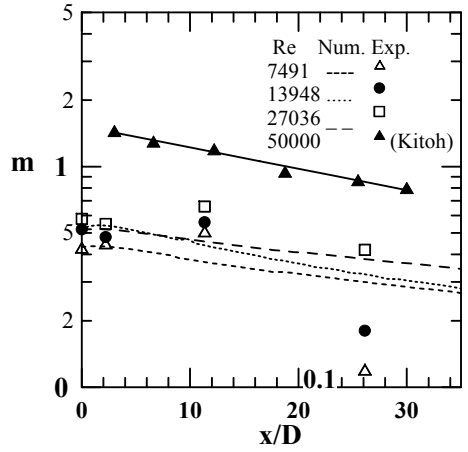

Figure 13. Decay of the swirl numbers at the pipe downstream.

CONCLUSIONS

The elliptic Navier-Stokes equations have been solved through a computer code developed. The computer code developed has been checked against two classical problems, solid body rotation and laminar source-sink flow, and, an excellent agreement has been obtained. Then, the turbulent flow in a circular pipe has been solved using the k-ε model. Finally, turbulent decaying swirl flow has been simulated. The obtained computational results have been validated by comparing them with the experimental results and a satisfactory agreement has been reached. The k-ε model has been disclosed to be an efficient model for the simulation of weak swirl turbulent flows. In addition, two pressure correction algorithms, SIMPLE and SIMPLEC, have been comparatively used and SIMPLEC has been shown to be superior to SIMPLE in terms of computing time.

REFERENCES

Bali, T., Modeling of Heat Transfer and Fluid flow for decaying Swirl Flow in a Circular Pipe, *Int. Comm. Heat Mass Transfer* 25, 3, 349-358, 1998.

Bali, T. and Ayhan, T., Experimental Investigation of Propeller Type Swirl Generator for a Circular Pipe Flow, *Int. Comm. Heat Mass Transfer* 26, 1, 13-22, 1999.

Chang, K.C., Chen, C.S. and Uang, C.I., A Hybrid k-ε Turbulence Model of Recirculating Flow, *Int. J. for Num. Meth. in Fluids* 12, 369-382, 1991.

Doormall, J.P. and Raithby, G.D., Enhancement of the SIMPLE Method for Predicting Incompressible Fluid Flows, *Numerical Heat Transfer* **7**, 147-163, 1984.

Hide, R., On source-sink flows in rotating fluid, *J. Fluid Mech*. 32, 737-745, 1968.

Hoekstra, A.J., Derksen, J.J. and Van Den Akker, H.E.A., An Experimental and Numerical Study of Turbulent Swirling Flow in Gas Cyclones, *Chemical Engineering Science* 54, 2055-2065, 1999.

Kitoh, D., Experimental study of turbulent swirling flow in a straight pipe, *J. Fluid Mech*. 225, 445-479, 1991.

Kreith, F. and Sonju, O.K., The Decay of a Turbulent Swirl in a Pipe, *J. Fluid Mech*. 22, 257-271, 1965.

Launder, B.E. and Spalding, D.B., The Numerical Computation of Turbulent Flows, *Comp. Meth. Appl. Mech. Eng* 3, 269-289, 1974.

Mondal, S., Datta, A. and Sarkar, A., Influence of Side Wall Expansion Angle and Swirl Generator on Flow Pattern in a Model Combustor Calculated with k-ε Model, *Int. J. of Thermal Science* 43, 9, 901-914, 2004.

Nikjooy, M. and Mongia, H.C., A 2nd Order Modeling Study of Confined Swirling Flow, *Int. J. Heat Fluid Flow,* 12, 1, 12-19, 1991.

Patankar, S.V., *Numerical Heat Transfer and Fluid Flow,* McGraw-Hill Book Co., New York, 1980.

Rodi, W., A Note on the Emprical Constant in the Kolmogorov-Prandtl Eddy Viscosity Expression, *ASME J. Fluids Eng* September, 386-389, 1975.

Sampers, W.F.J., Lamers, A.P.G.G. and Vansteenhoven, A.A., Analysis of Experimental and Numerical Results of a Turbulent Swirling Flow in a Tube, *Chemical Engineering Communications,* 125, 187-196, 1993.

Schlichting, H., *Boundary Layer Theory* (Seventh Ed.), McGraw-Hill Book Co., New York, 1979.

Senoo, Y. and Nagata, T., Swirl Flow in Long Pipes with Different Roughness, *Bulletin of JSME* 15, 1514-1521, 1972.

Smithberg, E. and Landis, F., Friction and Forced Convection Heat Transfer Characteristics in Tubes With Twisted Tape Swirl Generators, *ASME Journal of Heat Transfer* 86, 39-48, 1964.

Wang, P., Bai, X.S., Wessman, M., et al., Large Eddy Simulation and Experimental Studies of a Confined Turbulent Swirling Flow, *Physics of Fluids* 16, 9, 3306-3324, 2004.

Yang, Z.Y., Large Eddy Simulation of Fully Developed Turbulent Flow in a Rotating Pipe, *Int. J. for Numerical Methods In Fluids* 33, 5, 681-694, 2000.

Yrd.Doç.Dr. Tülin Bali, Karadeniz Teknik Üniversitesi Makina Mühendisliği Bölümü'nden 1985 yılında mezun oldu. 1988 yılında yüksek lisans ve 1994 yılında doktora derecelerini aldı. Çalışma alanı, sayısal ve deneysel ısı geçişi, ısı geçişinin iyileştirilmesi, ısıl sistemlerin performans analizi, vb. konuları kapsamaktadır. Evli ve 2 çocuk annesidir.